

# Human Mesenchymal Stem Cells Form Multicellular Structures in Response to Applied Cyclic Strain

ADELE M. DOYLE,<sup>1,2</sup> ROBERT M. NEREM,<sup>1,2</sup> and TABASSUM AHSAN<sup>1</sup>

<sup>1</sup>Parker H. Petit Institute for Biomedical Engineering and Biosciences, Georgia Institute of Technology, 315 Ferst Drive, Atlanta, GA 30332-0363, USA; and <sup>2</sup>Wallace H. Coulter Department of Biomedical Engineering, Georgia Institute of Technology/Emory University School of Medicine, 313 Ferst Drive, Suite 2127, Atlanta, GA 30332-0535, USA

(Received 22 February 2008; accepted 13 January 2009; published online 30 January 2009)

**Abstract**—Mesenchymal stem cells (MSCs) are a component of many cardiovascular cell-based regenerative medicine therapies. There is little understanding, however, of the response of MSCs to mechanical cues present in cardiovascular tissues. The objectives of these studies were to identify a model system to study the effect of well-defined applied cyclic strain on MSCs and to use this system to determine the effect of cyclic equibiaxial strain on the cellular and cytoskeletal organization of MSCs. When exposed to 10%, 1 Hz cyclic equibiaxial strain for 48 h, MSCs remained viable, retained characteristic gene and protein markers, and rearranged to form multicellular structures defined as clusters and knobs. This novel observation of cluster (overlapping cells surrounded by radial cellular projections) and knob (more dome-like structure containing significantly more cells than a cluster) formation did not involve changes in cytoskeletal proteins and resulted from cellular rearrangements initiated within 8 h of applied strain. Observed cellular responses were found to be dependent on substrate coating, but not on cell density for the 8-fold ranges tested. This system can thus be used to study the mechanoresponse over hours to days of MSCs exposed to applied cyclic strain in the context of cell–cell and cell–matrix interactions.

**Keywords**—Regenerative medicine, Mechanical forces, Cyclic strain, Mechanotransduction, Cytoskeleton, Cell–cell contact, Cell–matrix interaction.

## INTRODUCTION

Mesenchymal stem cells (MSCs) are one promising cell source option for cardiovascular cell-based regenerative medicine therapies. MSCs are currently involved in more than ten cardiovascular-related clinical trials world-wide, according to records in the NIH's clinical trials database. Published reports of completed clinical trials indicate MSCs may improve

cardiac function after stroke or myopathy.<sup>1,8,9,22,26,27,31</sup>

To support translational research efforts, recent *in vitro* studies have investigated several avenues by which MSCs may contribute to a potential therapy including: paracrine effects on resident cells and recruitment of additional cells,<sup>13,17,21,23,28,32</sup> local matrix remodeling,<sup>35</sup> and differentiation of the MSCs themselves along vascular smooth muscle-like<sup>2,16,31,42</sup> or endothelial-like<sup>29,31,43</sup> lineages. These previous and ongoing efforts signify growing interest from the clinical, translational, and basic science research communities in determining the potential of MSCs to contribute to cardiovascular therapies. These studies help address the need to more broadly and thoroughly determine the responses of MSCs to cardiovascular-relevant mechanical environments.

Mechanical forces are a major component of the vascular environment. Blood flow through vessels generates shear stress on the endothelial cell layer lining the lumen. Pulsatile contraction of the heart and large vessels causes changes in vessel diameter that generate cyclic strain on vessel tissue. Equibiaxial strain in particular has been used as an *in vitro* model for complex strains present in cardiac tissue<sup>30,34</sup> and large vessels such as the aorta<sup>4</sup> and pulmonary artery.<sup>6</sup> MSCs are expected to experience these mechanical cues if used in cardiovascular therapies, motivating further study to determine how this stem cell population will respond to these applied forces. Knowledge of the morphological and, ultimately, cell signaling changes elicited by applied mechanical force on MSCs will impact their contribution in cell-based regenerative medicine therapies.

The response of MSCs to applied physical forces has been studied mostly in the context of orthopaedics,<sup>5,15,18,20,36,39</sup> a natural initiation point given the source tissue. A subset of these studies have focused on tensile strain, though assessments concentrated on osteogenic differentiation.<sup>15,20,36</sup> Little work has been

Address correspondence to Tabassum Ahsan, Parker H. Petit Institute for Biomedical Engineering and Biosciences, Georgia Institute of Technology, 315 Ferst Drive, Atlanta, GA 30332-0363, USA. Electronic mail: adoyle@gatech.edu, robert.nerem@ibb.gatech.edu, taby@gatech.edu

done investigating the effect of cyclic tensile strain for vascular applications.<sup>25,30</sup> Further study is required, therefore, to more thoroughly characterize the mechanoresponse of MSCs to cyclic strain.

The study reported here was motivated by a need to better characterize the response of MSCs to cardiovascular-relevant mechanical forces. The objectives of these studies were to identify a model system to study the effect of well-defined applied cyclic strains on MSCs and to use this system to determine the effect of cyclic equibiaxial strain on the cellular and cytoskeletal organization of MSCs.

## METHODS

### *Materials*

The following reagents were purchased from Sigma (St. Louis, MO): low and high glucose Dulbecco's Modified Eagle's Medium (LG-DMEM, HG-DMEM), dexamethasone (DEX), ascorbic acid 2-phosphate (AA), beta-glycerophosphate ( $\beta$ -gly), indomethacin, 3-isobutyl-1-methylxanthine (IBMX), gelatin from porcine skin, donkey serum, FITC-conjugated anti-human IgG (Fc specific), and FITC-conjugated anti-human  $\alpha$ -smooth muscle actin. From Becton Dickinson (Bedford, MA), the following items were purchased: rat tail collagen type-I, mouse collagen type-IV, and PE-conjugated anti-human CD73. These items were purchased from Invitrogen (Carlsbad, CA): human plasma fibronectin, 0.05% trypsin/EDTA, AlexaFluor 546-conjugated phalloidin, and AlexaFluor 546-conjugated donkey anti-mouse IgG. Fetal bovine serum (FBS) for differentiation assays was purchased from Atlanta Biologicals (Lawrenceville, GA). Penicillin and streptomycin (P/S) was purchased from HyClone. Human recombinant insulin was purchased from Roche (Mannheim, Germany). For strain experiments, SILASTIC<sup>®</sup> BioMedical Grade Liquid Silicone Rubber was purchased from Specialty Manufacturing (Saginaw, MI) and O-Rings used to secure the silicone membrane to the membrane holder chamber were purchased from McMaster-Carr (Atlanta, GA). From Fitzgerald Industries International (Concord, MA), FITC-conjugated anti-human CD105 (Endoglin) and FITC-conjugated anti-mouse vimentin were purchased. The ligand for CD166, recombinant human CD6/Fc chimera, was purchased from R&D Systems (Minneapolis, MN). Mouse anti-human CD34 was purchased from Cell Signaling Technology (Danvers, MA). Mouse anti-rat CD45.2 was purchased from eBioscience (San Diego, CA). Mouse anti-human CD133 was purchased from Abgent (San Diego, CA). AlexaFluor 488-conjugated anti-mouse  $\alpha$ -tubulin was purchased from Millipore (Billerica, MA). Cy3-conjugated

donkey anti-mouse IgG was purchased from Jackson ImmunoResearch (West Grove, PA).

### *Cell Source and Culture*

Human adult bone marrow-derived MSCs and human adult aortic smooth muscle cells (SMCs) were obtained from Lonza (Walkersville, MD). MSCs and SMCs were expanded on tissue culture-treated polystyrene using vendor-distributed MSC Growth Medium (MSCGM) or SMC Growth Medium (SMCGM) for either 7 or 8 passages, respectively. To confirm the stem cell phenotype just prior to use, MSCs were assessed and found to have characteristic spindle-shaped morphology and protein expression, as well as differentiation potential<sup>3</sup> toward the osteogenic and adipogenic lineages (Supplemental Text and Figure).

### *Application of Strain*

A custom bioreactor was used to apply equibiaxial cyclic strain to cell-seeded silicone membranes, as previously published.<sup>4,38</sup> To prepare for cell seeding, silicone surfaces were coated with extracellular matrix proteins using an established method.<sup>4,11,40,41</sup> Briefly, silicone membranes were etched in 1N H<sub>2</sub>SO<sub>4</sub> for 20 min prior to sterilization; subsequently 3 mL of protein solution was allowed to adsorb in a defined 10 cm<sup>2</sup> area for 2 h at 37 °C. Final protein concentrations were 1% gelatin or 5  $\mu$ g/cm<sup>2</sup> of collagen type I, collagen type IV, or fibronectin. MSCs or SMCs were then seeded in the center at densities ranging from 1000 to 64,000 cells/cm<sup>2</sup> using 2 mL of MSCGM or SMCGM, respectively, and allowed to adhere for 48 h at 37 °C/5% CO<sub>2</sub>. Medium (25 mL) was then added to each sample and experimental samples were exposed to equibiaxial cyclic strain (10.3  $\pm$  0.2% imposed area change, 1.00  $\pm$  0.02 Hz) for up to 48 h. Parallel control samples were cultured under static conditions.

### *Cell Viability*

Cell viability was visualized using LIVE/DEAD Viability/Cytotoxicity staining (Invitrogen, Carlsbad, CA), with live and dead cells fluorescently labeled with green or red, respectively. To quantify percent viability, cells were trypsinized off silicone surfaces and analyzed in a ViCELL Cell Viability Analyzer (Beckman Coulter, Fullerton, CA), an automated system to assess trypan blue exclusion.

### *Flow Cytometry*

Expression of surface proteins was detected by staining cells with fluorescence-conjugated antibodies

and using a flow cytometer (LSR, Becton Dickinson, Franklin Lakes, NJ). For characterization of MSCs, surface markers CD73, CD105, CD166 (detected using the ligand CD6), CD34, CD45.2, and CD133 were used to assess the protein expression profile of cells. Cells were first trypsinized off culture surfaces, fixed with 4% formaldehyde for 15 min at 4 °C, and stored in working buffer solution (WBS; 0.3% BSA/0.001% Tween-20 in PBS with calcium and magnesium) at 4 °C until further analysis. Samples were blocked for non-specific binding using a 10% donkey serum solution for 1 h at 4 °C. Each sample was then divided, with one half incubated with WBS (cell only control) and the other with primary and, if necessary, secondary antibody (1/100 dilution in WBS) for 30 min at 4 °C. A minimum of 20,000 events were analyzed using the cytometer to generate a histogram of fluorescence.

### *Cell Imaging*

Phase images of samples cultured on tissue culture plastic or silicone were taken on an Axiovert 200 microscope (Zeiss, Thornwood, NY). Some samples were fixed on the silicone membrane using 4% formaldehyde for 5 min at room temperature in preparation for subsequent fluorescent staining of cytoskeletal elements and visualization of cell patterning. Microfilaments were visualized by staining with phalloidin per manufacturer-provided instructions. Intermediate filaments and microtubules were assessed using immunocytochemical staining for anti-vimentin and anti- $\alpha$ -tubulin, respectively. At room temperature, immunocytochemical samples were permeabilized with 0.05% Triton X-100 for 5 min, blocked with 5% donkey serum (Sigma, St. Louis, MO) for 30 min, stained with antibody (1/100 dilution) for 2 h, and washed with PBS. Hoechst 33258 (Invitrogen, Carlsbad, CA) counterstain was added to indicate cell nuclei. Samples were visualized using a fluorescent (Eclipse E600, Nikon, Melville, NY) or confocal (LSM 510, Zeiss, Thornwood, NY) microscope. Average cell number per cluster or knob was determined from the fluorescent samples, manually counting cells in all knobs (maximum 15 observed per sample) and up to 10 clusters per stained sample from three independent experiments.

### *Gene Expression Analysis*

Expression of a characteristic MSC surface marker, CD73, and an early SMC differentiation gene,  $\alpha$ -smooth muscle actin (a-SMA), was quantified in strain and static samples by Real-Time PCR (qRT-PCR). Cell lysates were harvested from samples following 24 h strain (10%, 1 Hz) or parallel static culture on

gelatin-coated silicone. Total RNA was harvested from cell lysates according to manufacturer's recommendation (RNeasy kit, Qiagen). RNA was quantified using a NanoDrop (Thermo Scientific) and 1  $\mu$ g RNA was then used as a template to reverse transcribe cDNA (SuperScript III First-Strand Synthesis System, Invitrogen). qRT-PCR was completed using an 800 nM primer concentration (CD73 Forward: GGTATCCG GTCGCCATT; CD73 Reverse: GCCTCCAAAGG GCAATACAG; a-SMA Forward: CAAGTGATCAC CATCGGAAATG; a-SMA Reverse: GACTCCAT CCCGATGAAGGA) and Power SYBR Green Mastermix (ABI) on a StepOnePlus Real-Time PCR instrument (ABI).

### *Statistical Analysis*

Statistical significance was determined using a two-way t-test. Data are represented as average  $\pm$  standard error of the mean.

## **RESULTS**

### *MSC Response to Equibiaxial Applied Strain*

Mesenchymal stem cells were exposed to equibiaxial strain and assessed for cellular changes. Cells seeded at 8000 cells/cm<sup>2</sup> on gelatin-coated silicone and subjected to 10% strain at 1 Hz for 48 h were assessed for viability and expression of surface proteins. Fluorescent images of samples assessed for viability showed that almost all cells in both static (Fig. 1a) and strain (Fig. 1b) samples were live (indicated in green), with few to no apparent dead cells (red). Assessment of the attached cells indicated that they continued to have an MSC phenotype, as both static (green) and strain (red) samples expressed markedly higher levels of CD73 and CD105 (Fig. 1, graph), compared to unstained controls (black fill). Fewer total attached cells, however, were recovered from strain samples relative to static controls ( $108 \pm 18$  vs.  $232 \pm 08$  E4 cells, respectively;  $p < 0.005$ ,  $n = 4$ ). Analysis of the media for particles 5–50  $\mu$ m indicated  $< 5$  E4 counts per static sample vs.  $196 \pm 36$  E4 per strain sample ( $p < 0.005$ ,  $n = 4$ ). Notably, 86% of suspended particles in strain samples were  $< 10 \mu$ m, while the average cell size of attached MSCs was  $15.9 \pm 0.8 \mu$ m. In summary, the viability of attached MSCs is high for both static and strain samples, although samples subjected to strain released markedly higher amounts of debris, potentially including cell fragments, into the medium.

Cells seeded at 8000 cells/cm<sup>2</sup> on gelatin-coated silicone were subjected to 10%, 1 Hz cyclic equibiaxial strain for up to 48 h (Figs. 1–4). At 48 h, statically cultured and strained samples were stained for F-actin

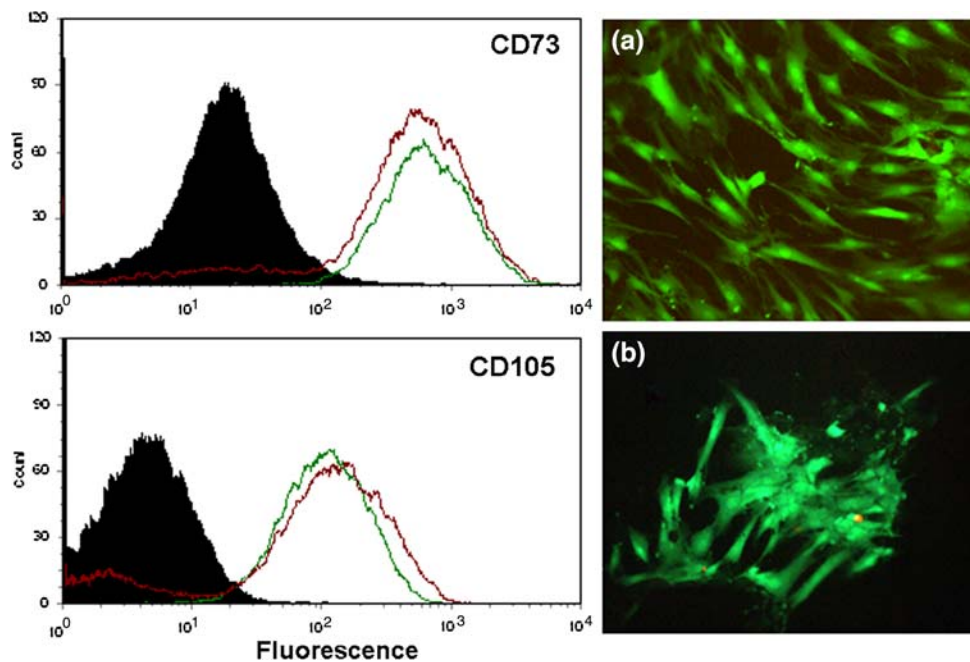


**FIGURE 1.** MSC viability and protein expression after cyclic equibiaxial strain. Static control (a) and experimental strain (b; 10%, 1 Hz, 48 h, gelatin-coated silicone) samples both consisted predominantly of live (green) cells, with few to no attached dead (red) cells. Images taken at 200 $\times$ . Expression of characteristic MSC protein markers CD73 and CD105 were equally expressed in strained (red) and static (green) controls (unstained controls shown in solid black).

to visualize cell distribution and arrangement. In static controls, cells were confluent and randomly oriented (Fig. 2: left-most column), similar to MSCs expanded on tissue culture plastic. In strained samples, some isolated single cells (Fig. 2: 2nd column from left) were also randomly oriented. More noticeable, however, were many multicellular three-dimensional structures. These structures were categorized as clusters (Fig. 2: 3rd column from left, Fig. 3a) or knobs (Fig. 2: right-most column, Fig. 3b).

Cluster and knob categories were defined based on cell arrangement and then assessed for differences in cell number and cytoskeletal protein expression. Clusters were defined as multicellular units of cells, dense in the center with thin processes extending radially outward from the center. Knobs, also defined as multicellular three-dimensional structures, were highly refractive under phase illumination with densely packed dome-like regions sitting atop an adherent cell layer beneath. Knobs had a smooth exterior surface and appeared denser in terms of nuclei per projected surface area (Fig. 3b). Both clusters and knobs usually occurred as isolated units, clearly distinct from neighboring structures. Within a single sample, clusters appeared more frequently than knobs, but most samples contained examples of both structures. The number of cells per structure was determined by fluorescently staining cell nuclei with Hoechst 33258 and imaging through the  $z$ -plane on a confocal microscope.

Due to the more consistent appearance of clusters in all samples, only 10 clusters, but up to 15 knobs, were counted per sample. Consistent with qualitative indication of differences in nuclear density, knobs were found to have significantly ( $p = 0.05$ ,  $n \geq 33$ ) more cells than clusters,  $54 \pm 35$  vs.  $35 \pm 23$  cells, respectively (Fig. 3).

Cytoskeletal patterning was assessed in strain and static samples by visualizing microfilaments (phalloidin stain for F-actin or  $\alpha$ -SMC actin immunocytochemistry), intermediate filaments (vimentin immunocytochemistry), and microtubules ( $\alpha$ -tubulin immunocytochemistry). In both static controls and strained samples, microfilaments were present throughout and aligned parallel to the major axis of the elliptical cell (Fig. 2). Clusters and, in particular, knobs, contained regions of intense phalloidin fluorescence near the center of the multicellular structure. Assessment methods available for these studies, however, could not visually resolve whether areas of increased staining resulted from a change in the filament properties within a single cell or from the overlapping of multiple cells. Flow cytometry analysis for  $\alpha$ -SMC actin also found no detectable quantitative difference in microfilament expression levels between static controls and strained samples. Vimentin staining of clusters and knobs (Fig. 3a and b, respectively) showed thin intermediate filaments aligned circumferentially around the nucleus. Neither vimentin nor  $\alpha$ -tubulin (not shown)

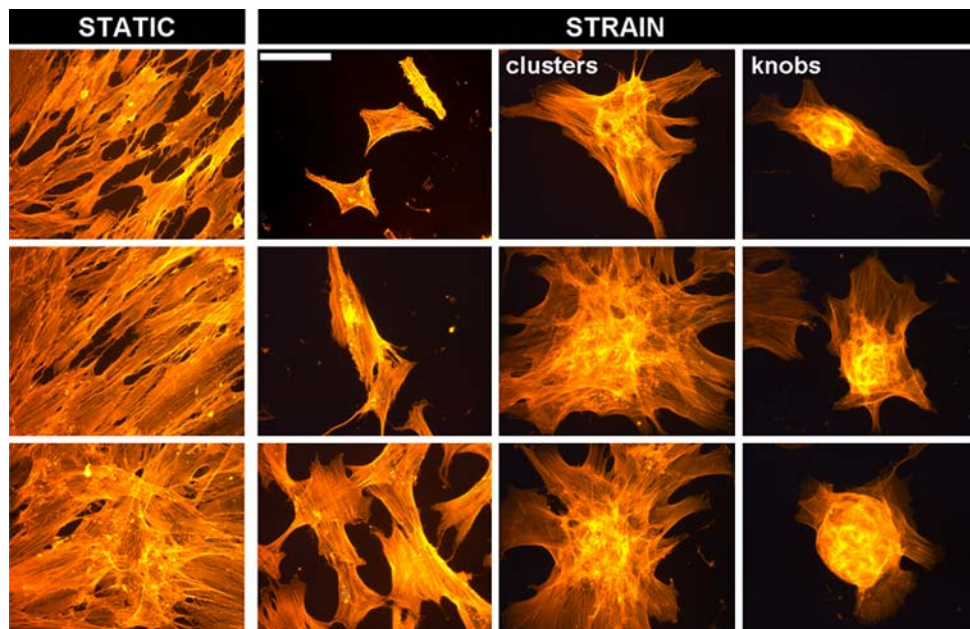


**FIGURE 2.** Cellular arrangements in response to strain. Three representative images of phalloidin-stained samples per column indicate the different categories of cellular arrangements. In static samples (left-most column), cells are arranged randomly. In response to cyclic equibiaxial strain (10%, 1 Hz, 48 h), some single cells are also arranged randomly (2nd column from left). Unique to the strain samples, three-dimensional multi-cellular structures form that have been categorized as clusters (3rd column from left) or knobs (right-most column). Scale bar = 200  $\mu\text{m}$ .

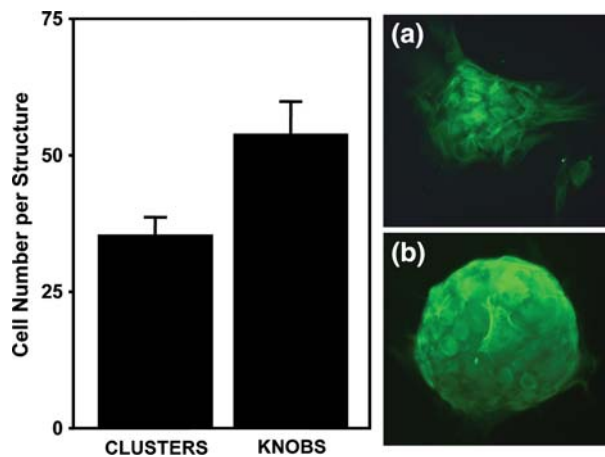


**FIGURE 3.** Characteristics of clusters and knobs. Vimentin-stained images indicate the arrangement of cells within a cluster (a) and knob (b). Clusters are multicellular three-dimensional structures with cell processes radially projecting from the center. Knobs are also multicellular and three-dimensional, but are more highly refractive dome-like structures. Quantitation of the number of the cells per structure showed significantly ( $p < 0.05$ ) more in knobs ( $n = 33$ ) compared to clusters ( $n = 49$ ). Images taken at 200 $\times$ .

staining revealed differences in patterning between strain and static samples. Overall for all three filament types, cytoskeletal arrangement showed no visually marked difference in total number, spatial organization, or thickness of filaments within a cell, when

comparing either individual clusters vs. knobs or overall statically cultured vs. strained samples.

The kinetics of cluster and knob formation was determined by taking phase images at intervals of samples seeded at 8000 cells/cm<sup>2</sup> on gelatin-coated silicone and then cultured statically or subjected to 10%, 1 Hz cyclic equibiaxial strain for up to 48 h. Images taken at the start of treatment (after 48 h of attachment), and then 8, 12, 24, 36, and 48 h later of static controls and strained samples are shown in Fig. 4. Taken together, the series of images indicate that in response to cyclic strain, there is initial cellular rearrangement into groups of a few cells within 8 h, as distinct from the random cell distribution in static controls (Fig. 4, b vs. a). Furthermore, small clusters are already distinguishable at 12 h (Fig. 4, d vs. c), though knobs are only apparent after 36 h (Fig. 4, h vs. g). After 48 h, strain samples are markedly different than parallel static controls (Fig. 4i) and consist of isolated single cells, clusters (Fig. 4j<sub>1</sub>), and knobs (Fig. 4j<sub>2</sub>). Once developed, the MSC multicellular structures observed on gelatin-coated silicone in response to cyclic strain for 48 h continue to persist for up to 6 days. Furthermore, as shown in these studies (Fig. 4, SMCs) and by others,<sup>19</sup> similar structures are seen in SMC cultures seeded at a similar initial cell density on the same substrate, but cultured under static conditions. Major shifts in phenotype, however, are not required for the formation of these MSC

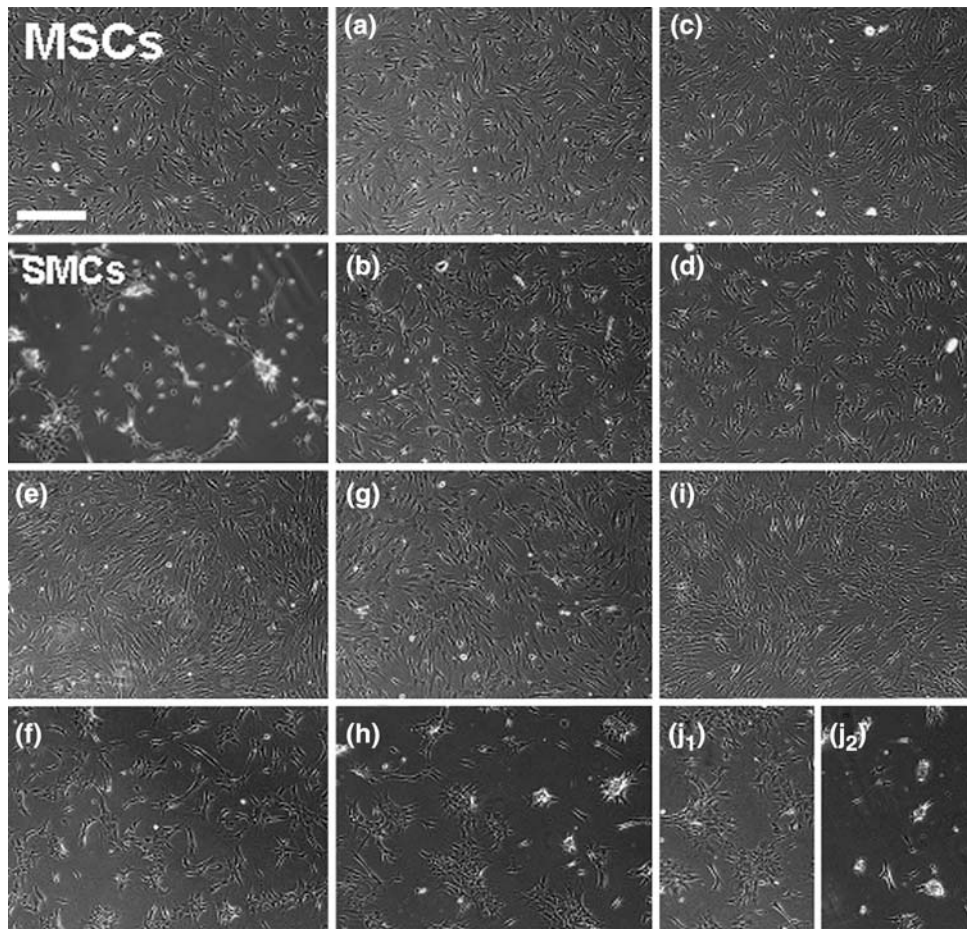


**FIGURE 4.** Kinetics of MSC rearrangement in response to strain. Phase images of MSCs immediately prior to treatment (MSCs), and subsequently cultured under static (a, c, e, g, i) or strain (b, d, f, h, j; 10%, 1 Hz, gelatin-coated silicone) conditions. Images were taken after 8 (a–b), 12 (c–d), 24 (e–f), 36 (g–h), and 48 (i–j) hours. Early signs of cellular rearrangement are seen at 8 h (b vs. a), with clusters and knob formation apparent by 36 h (h vs. g). After 48 h, distinct clusters ( $j_1$ ) and knobs ( $j_2$ ) are present within a single sample. Structures are also seen in smooth muscle cell cultures seeded at a similar initial cell density on the same substrate, but cultured under static conditions (SMCs). Scale bar = 400  $\mu\text{m}$ .

multicellular structures, as after 24 h of applied strain there was no significant change in gene expression of key MSC (CD73:  $p = 0.287$ ,  $n = 4$ ) and SMC ( $\alpha$ -SMA:  $p = 0.727$ ,  $n = 4$ ) markers between static and strain samples.

#### *Substrate Dependency of MSC Response to Strain*

The effect of surface proteins on the response of MSCs (8000 cells/cm<sup>2</sup> initial seeding density) to cyclic strain (10%, 1Hz, 48 h) was determined by using various matrix substrates. On collagen type I-coated surfaces, MSCs subjected to strain rearranged to form clusters and knobs (Fig. 5b), as was seen on gelatin-coated silicone here (Fig. 5a) and previously (Figs. 2–4). In contrast, MSCs cultured on collagen type IV- or fibronectin-coated silicone and subjected to strain (Fig. 5c–d) looked confluent and not dissimilar to parallel static controls (not shown).

#### *Cell Density Effects on MSC Response to Strain*

The effect of cell density on cluster and knob formation was also investigated. This was particularly important due to slight variations in confluency after the 48 h adhesion duration (just prior to treatment) for samples on different protein substrates. Cells seeded at 8000 cells/cm<sup>2</sup> were significantly ( $p < 0.001$ ,  $n = 4$ ) more confluent on fibronectin-coated silicone compared to gelatin-coated silicone samples ( $14.5 \pm 1.2$  vs.  $8.9 \pm 1.1 \cdot 10^3$  cells/cm<sup>2</sup>) after 48 h. To determine whether this altered initial cell density at the time of applied strain was responsible for differences in strain-responsive cellular rearrangements, cells were seeded on fibronectin- or gelatin-coated silicone at lower or higher densities, respectively, and subjected to the same cyclic strain used previously. Phase images of static (Fig. 6a, c) and strain (Fig. 6b, d) samples seeded at 1000 (Fig. 6a, b) or 4000 cells/cm<sup>2</sup> (Fig. 6c, d) on fibronectin-coated

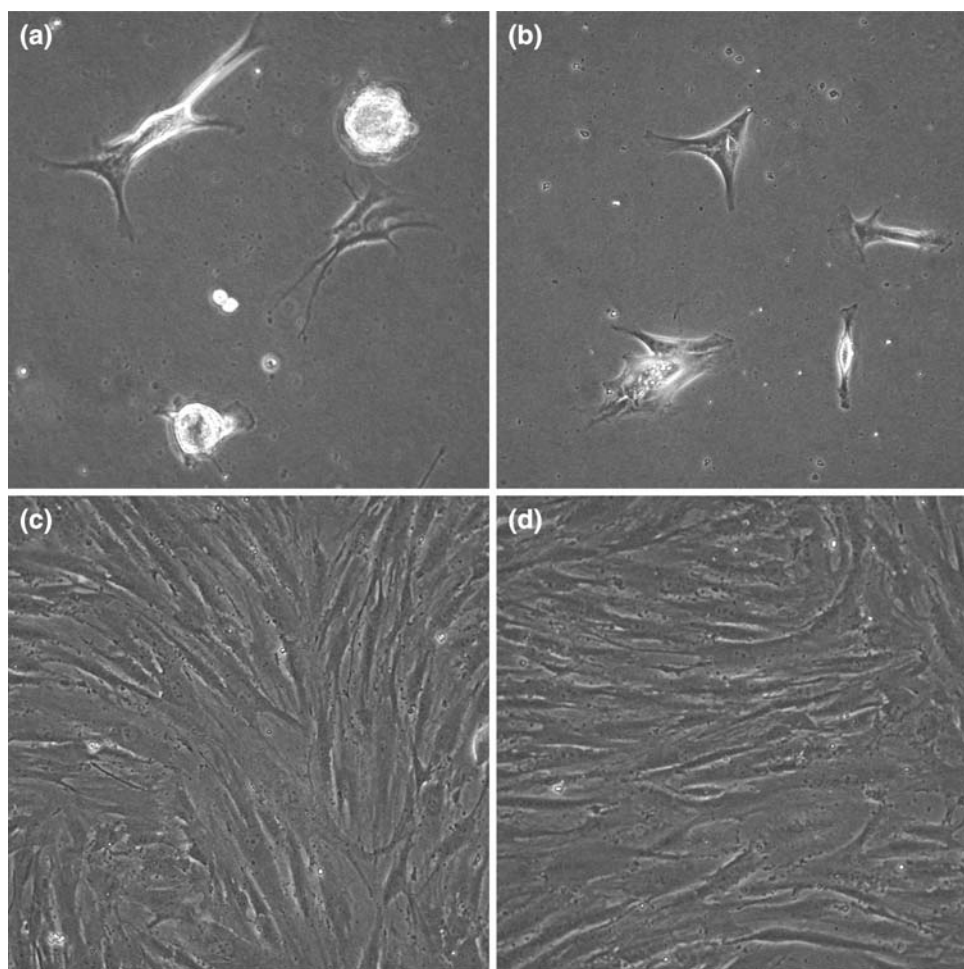


**FIGURE 5.** Substrate dependency of cellular arrangements in response to strain. Phase images of MSCs strained (10%, 1 Hz, 48 h) after seeding at 8000 cells/cm<sup>2</sup> on silicone coated with gelatin (a); collagen type I (b); collagen type IV (c); or fibronectin (d). MSCs strained on gelatin- or collagen type I-coated surfaces remodeled into multicellular clusters, while MSCs on collagen type IV- or fibronectin-coated surfaces showed no marked rearrangement. In all parallel static controls, cells remained randomly oriented (not shown). Images taken at 200 $\times$ .

silicone did not reveal any difference in cell rearrangement after 48 h strain. Samples cultured on gelatin-coated surfaces at 16,000, 32,000, or 64,000 cells/cm<sup>2</sup> all showed rearrangement of MSCs in response to strain (data not shown), similar to the cluster and knob formation described previously for samples seeded at 8000 cells/cm<sup>2</sup>. Despite increased proliferation on fibronectin, the samples with the highest cell density on gelatin ( $61.55 \pm 1.11$  E3 cells/cm<sup>2</sup> just prior to strain) still had structures, while those with the lowest density on fibronectin ( $2.32 \pm 0.64$  E3 cells/cm<sup>2</sup>) did not. Thus, an 8-fold change in initial seeding density on a given substrate did not alter the response outcome of cellular rearrangement to strain.

## DISCUSSION

Mesenchymal stem cells seeded on gelatin-coated silicone and exposed to 10%, 1 Hz cyclic equibiaxial

strain for 48 h remained viable, retained key MSC surface markers, and rearranged to form multicellular structures defined as clusters and knobs. This novel observation of cluster (overlapping cells surrounded by radial cellular projections) and knob (more dome-like structure containing significantly more cells than clusters) formation did not involve changes in cytoskeletal protein concentration or organization and resulted from cellular rearrangements initiated within 8 h of applied strain. Observed cellular responses were found to be dependent on substrate coating, but not on cell density for the 8-fold ranges tested. This system can thus be used to study the mechanoreponse over hours to days of MSCs to applied cyclic strain in the context of cell–cell and cell–matrix interactions.

Cellular rearrangement has been shown to be a mechanoreponse of MSCs to cyclic strain. When subjected to uniaxial cyclic strain, MSCs reorient to be perpendicular to the axis of stretch within 1 day.<sup>30</sup> It is

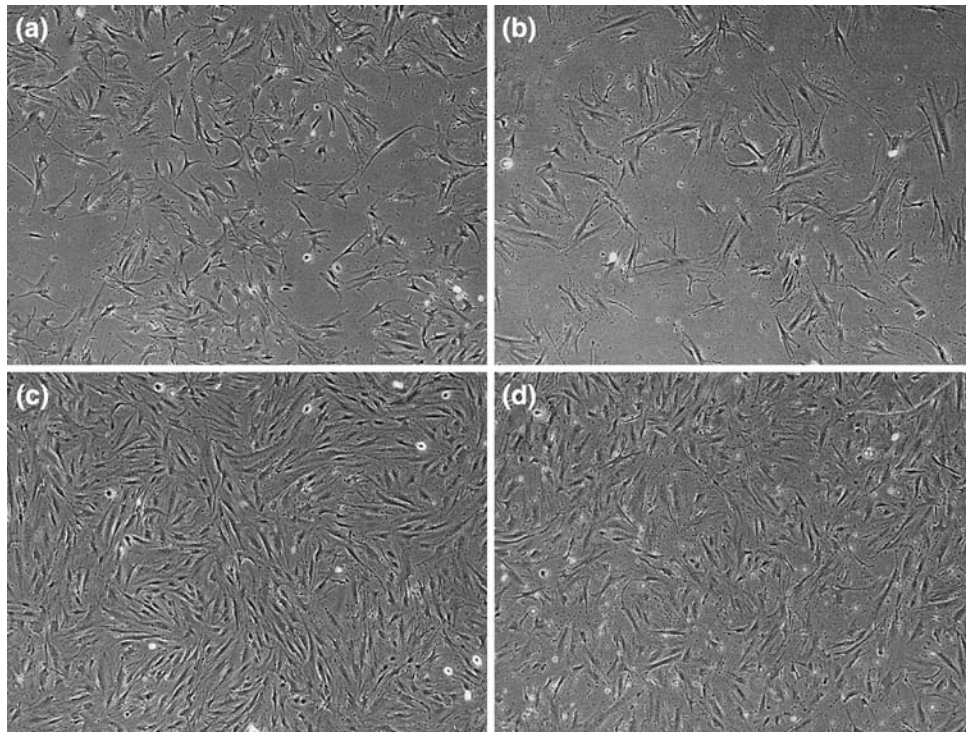


**FIGURE 6.** Effect of seeding density on cellular arrangements in response to strain. Phase images of MSCs seeded at as low as 1000 (a, b) or 4000 (c, d) cells/cm<sup>2</sup> on fibronectin-coated silicone and cultured under static (a, c) or strain (10%, 1 Hz, 48 h) (b, d) conditions indicated no marked cellular rearrangements. Images taken at 50 $\times$ .

postulated that this response is to minimize the effective strain sensed by the cells. This is consistent with the diminished gene changes observed as MSCs align in response to strain<sup>30</sup> or when lithography is used to pre-align MSCs perpendicular to the single axis of strain.<sup>25</sup> Equibiaxial strain, which generates strain in both the radial and circumferential directions, does not provide a perpendicular axis on the surface to which cells could align and thus presents a continual mechanical cue over time. Using an equibiaxial system, some studies have investigated the effects of cyclic strain on intracellular signaling pathways<sup>36</sup> and proliferation.<sup>37</sup> Another study,<sup>30</sup> using the same magnitude (10%) and frequency (1 Hz) of cyclic equibiaxial strain and assessing for similar cellular arrangements as in our studies, did not observe clusters and knobs. Differences in the type and manner of protein coating most likely account for these differences, given the sensitivity of structure formation to the underlying substrate.

The application of cyclic equibiaxial strain resulted in a heterogeneous distribution of cells. Prior to the application of strain, samples consisted of a homogeneous monolayer of MSCs. With changes in cellular arrangement grossly visible by 8 h, the initial mechanoreponse was not dependent on a phenotypic shift within the cells. It was not determined in these studies, however, whether the ultimate heterogeneity in

distribution is associated with heterogeneity in cell characteristics, nor whether structure formation is due to or results from those differences. Nonetheless, the persistence of both clusters and knobs at 6 days of culture implies that these structures are not stages within a single process, but rather a result of distinct cues at the microenvironment level. While the primary mechanical cue applied to the MSCs is equibiaxial cyclic strain, concomitant changes in the stiffness of the underlying membrane<sup>14</sup> and shear due to fluid motion<sup>38</sup> may affect the cellular microenvironment.

The model system developed in these studies can be used to better characterize the mechanoreponse of MSCs to applied cyclic strain. Though there have been a few studies<sup>30,36,37</sup> looking at the response of MSCs to cyclic equibiaxial strain, there has not been a methodical approach to investigate the effects of mechanical parameters (e.g., strain magnitude, frequency, and duty cycle) on cellular processes. With changes in cellular arrangement noticeable within hours and persistent for days, this model system can be used to assess both short term mechanoreponses in cell behavior (e.g., proliferation and migration) and intracellular signaling, and long term responses such as matrix synthesis and differentiation.

Our results indicate that the mechanoreponse of MSCs is mitigated by other environmental cues,



including cell–cell and cell–matrix interactions. In studies focused on SMCs, cyclic strain has been shown to affect the expression and localization of focal contact components.<sup>10</sup> Recent work in MSCs has shown that cell–cell interactions can span up to hundreds of microns,<sup>44</sup> having an effect not only on neighboring cells but more distant cells. Thus, the need to determine the effects of cell–cell communication on the mechanoresponse to cyclic strain is still important in these cultures with a heterogeneous distribution of cells.

Cell-attachment mechanisms are important in regulating MSC behavior. In static cultures *in vitro*, MSC binding to polymer scaffolds via distinct ligands resulted in differential gene expression.<sup>7</sup> Functionalized glass surfaces have been used to favor specific differentiation pathways,<sup>12</sup> while electrically charging substrates can affect cell attachment and spreading.<sup>33</sup> *In vivo*, integrins have been implicated in trafficking and homing of MSCs in ischemic myocardium. Thus, the substrate-dependent mechanoresponse to cyclic strain in our system may be mediated by cell-attachment mechanisms, such as distinct integrin subunits, activated by the different protein coatings. As a result, future strain studies need to be meticulous in both the type and form of protein presentation.

The role of proliferation in formation or maintenance of the multicellular structures was not directly assessed in this study. However, the limited difference between the theoretical cell number seeded (8000 cells/cm<sup>2</sup>) and that present immediately prior to the application of strain (~8900 cells/cm<sup>2</sup>) indicates that the overall population of MSCs on gelatin-coated silicone may not significantly proliferate during the 48-h period of applied strain. Furthermore, the persistence of multicellular structures for up to 6 days following the application of cyclic strain, with no apparent change in size or morphology, suggests that there is no net proliferation of cells in multicellular structures.

The existence of cyclic tensile strains in tissues *in vivo* has motivated studies related to differentiation of MSCs. Multiple cyclic strain profiles have been shown to promote osteogenic and chondrogenic differentiation,<sup>15,20</sup> even in the absence of differentiating growth factors.<sup>39</sup> A few vascular studies have investigated the effects of cyclic strain on SMC gene and protein expression.<sup>24,30</sup> Preliminary gene expression assessments in this study suggest that during the first 24 h of applied strain, MSCs do not deviate from an MSC phenotype, based on maintenance of CD73 expression and no increase in  $\alpha$ -SMA expression. Longer (>1 week) term studies would likely be necessary to determine whether MSCs have the potential to differentiate into SMCs. These studies, however, indicate that undifferentiated MSCs may be capable of

certain functions similar to those of SMCs, as may be beneficial in certain vascular cell-based therapies.

These studies show that MSCs subjected to cyclic equibiaxial strain form multiple variants of complex multicellular structures. The mechanoresponse of MSCs is dependent on the underlying protein substrate and involves changes observable within hours. We have shown that this model system of cyclic strain can be used to investigate the short (hours) and long (days) term mechanoresponses of MSCs in the context of cell–cell and cell–matrix interactions. Future studies also need to focus on a systematic analysis of the effect of mechanical parameters, including magnitude and frequency, on the mechanoresponse of stem cells to tensile strain.

## ELECTRONIC SUPPLEMENTARY MATERIAL

The online version of this article (doi:[10.1007/s10439-009-9644-y](https://doi.org/10.1007/s10439-009-9644-y)) contains supplementary material, which is available to authorized users.

## ACKNOWLEDGMENTS

The authors thank the Georgia Tech/Emory Center for the Engineering of Living Tissues (National Science Foundation Engineering Research Center: NSF EEC-9731643; AMD, RMN, TA), the Ruth L. Kirschstein National Research Service Award (1F32HL076978-01A1; TA), the NIH Cellular and Tissue Engineering Training Program (5T32GM008433-14 and 5T32GM008433-15; AMD), and the Georgia Institute of Technology President's Fellowship (AMD) for financial support. This material is based upon work supported under a National Science Foundation Graduate Research Fellowship (AMD). Thanks to Garry Duffy for protocols related to the differentiation of MSCs. There are no conflicts of interest for the authors to disclose.

## REFERENCES

- <sup>1</sup>Arguero, R., G. Careaga-Reyna, R. Castano-Guerra, M. H. Garrido-Garduno, J. A. Magana-Serrano, and M. de Jesus Nambo-Lucio. Cellular autotransplantation for ischemic and idiopathic dilated cardiomyopathy. Preliminary report. *Arch. Med. Res.* 37:1010–1014, 2006. doi:[10.1016/j.arcmed.2006.05.012](https://doi.org/10.1016/j.arcmed.2006.05.012).
- <sup>2</sup>Ball, S. G., A. C. Shuttleworth, and C. M. Kielty. Direct cell contact influences bone marrow mesenchymal stem cell fate. *Int. J. Biochem. Cell. Biol.* 36:714–727, 2004. doi:[10.1016/j.biocel.2003.10.015](https://doi.org/10.1016/j.biocel.2003.10.015).
- <sup>3</sup>Barry, F. P., and J. M. Murphy. Mesenchymal stem cells: clinical applications and biological characterization. *Int. J.*

- Biochem. Cell. Biol.* 36:568–584, 2004. doi:10.1016/j.biocel.2003.11.001.
- <sup>4</sup>Butcher, J. T., B. C. Barrett, and R. M. Nerem. Equibiaxial strain stimulates fibroblastic phenotype shift in smooth muscle cells in an engineered tissue model of the aortic wall. *Biomaterials* 27:5252–5258, 2006. doi:10.1016/j.biomaterials.2006.05.040.
- <sup>5</sup>Campbell, J. J., D. A. Lee, and D. L. Bader. Dynamic compressive strain influences chondrogenic gene expression in human mesenchymal stem cells. *Biorheology* 43:455–470, 2006.
- <sup>6</sup>Chaqour, B., P. S. Howard, C. F. Richards, and E. J. Macarak. Mechanical stretch induces platelet-activating factor receptor gene expression through the NF-kappaB transcription factor. *J. Mol. Cell. Cardiol.* 31:1345–1355, 1999. doi:10.1006/jmcc.1999.0967.
- <sup>7</sup>Chastain, S. R., A. K. Kundu, S. Dhar, J. W. Calvert, and A. J. Putnam. Adhesion of mesenchymal stem cells to polymer scaffolds occurs via distinct ECM ligands and controls their osteogenic differentiation. *J. Biomed. Mater. Res. A* 78:73–85, 2006. doi:10.1002/jbm.a.30686.
- <sup>8</sup>Chen, S. L., W. W. Fang, J. Qian, F. Ye, Y. H. Liu, S. J. Shan, J. J. Zhang, S. Lin, L. M. Liao, and R. C. Zhao. Improvement of cardiac function after transplantation of autologous bone marrow mesenchymal stem cells in patients with acute myocardial infarction. *Chin. Med. J. (Engl)*. 117:1443–1448, 2004.
- <sup>9</sup>Chen, S. L., W. W. Fang, F. Ye, Y. H. Liu, J. Qian, S. J. Shan, J. J. Zhang, R. Z. Chunhua, L. M. Liao, S. Lin, and J. P. Sun. Effect on left ventricular function of intracoronary transplantation of autologous bone marrow mesenchymal stem cell in patients with acute myocardial infarction. *Am. J. Cardiol.* 94:92–95, 2004. doi:10.1016/j.amjcard.2004.03.034.
- <sup>10</sup>Cunningham, J. J., J. J. Linderman, and D. J. Mooney. Externally applied cyclic strain regulates localization of focal contact components in cultured smooth muscle cells. *Ann. Biomed. Eng.* 30:927–935, 2002. doi:10.1114/1.1500408.
- <sup>11</sup>Cunningham, J. J., J. Nikolovski, J. J. Linderman, and D. J. Mooney. Quantification of fibronectin adsorption to silicone-rubber cell culture substrates. *Biotechniques* 32:876, 878, 880 passim, 2002.
- <sup>12</sup>Curran, J. M., R. Chen, and J. A. Hunt. The guidance of human mesenchymal stem cell differentiation in vitro by controlled modifications to the cell substrate. *Biomaterials* 27:4783–4793, 2006. doi:10.1016/j.biomaterials.2006.05.001.
- <sup>13</sup>Dai, W., S. L. Hale, B. J. Martin, J. Q. Kuang, J. S. Dow, L. E. Wold, and R. A. Kloner. Allogeneic mesenchymal stem cell transplantation in postinfarcted rat myocardium: short- and long-term effects. *Circulation* 112:214–223, 2005. doi:10.1161/CIRCULATIONAHA.104.527937.
- <sup>14</sup>Engler, A. J., S. Sen, H. L. Sweeney, and D. E. Discher. Matrix elasticity directs stem cell lineage specification. *Cell* 126:677–689, 2006. doi:10.1016/j.cell.2006.06.044.
- <sup>15</sup>Friedl, G., H. Schmidt, I. Rehak, G. Kostner, K. Schauenstein, and R. Windhager. Undifferentiated human mesenchymal stem cells (hMSCs) are highly sensitive to mechanical strain: transcriptionally controlled early osteo-chondrogenic response in vitro. *Osteoarthr. Cartil.* 15:1293–1300, 2007. doi:10.1016/j.joca.2007.04.002.
- <sup>16</sup>Gong, Z., and L. E. Niklason. Small-diameter human vessel wall engineered from bone marrow-derived mesenchymal stem cells (hMSCs). *Faseb J.* 22:1635–1648, 2008.
- <sup>17</sup>Gruber, R., B. Kandler, P. Holzmann, M. Vogele-Kadletz, U. Losert, M. B. Fischer, and G. Watzek. Bone marrow stromal cells can provide a local environment that favors migration and formation of tubular structures of endothelial cells. *Tissue Eng.* 11:896–903, 2005. doi:10.1089/ten.2005.11.896.
- <sup>18</sup>Huang, C. Y., K. L. Hagar, L. E. Frost, Y. Sun, and H. S. Cheung. Effects of cyclic compressive loading on chondrogenesis of rabbit bone-marrow derived mesenchymal stem cells. *Stem Cells* 22:313–323, 2004. doi:10.1634/stemcells.22-3-313.
- <sup>19</sup>Hubschmid, U., P. M. Leong-Morgenthaler, A. Basset-Dardare, S. Ruault, and P. Frey. In vitro growth of human urinary tract smooth muscle cells on laminin and collagen type I-coated membranes under static and dynamic conditions. *Tissue Eng.* 11:161–171, 2005. doi:10.1089/ten.2005.11.161.
- <sup>20</sup>Jagodzinski, M., M. Drescher, J. Zeichen, S. Hankemeier, C. Krettek, U. Bosch, and M. van Griensven. Effects of cyclic longitudinal mechanical strain and dexamethasone on osteogenic differentiation of human bone marrow stromal cells. *Eur. Cell Mater.* 7:35–41, 2004; discussion 41.
- <sup>21</sup>Kasper, G., N. Dankert, J. Tuischer, M. Hoefl, T. Gaber, J. D. Glaeser, D. Zander, M. Tschirschmann, M. Thompson, G. Matziolis, and G. N. Duda. Mesenchymal stem cells regulate angiogenesis according to their mechanical environment. *Stem Cells* 25:903–910, 2007. doi:10.1634/stemcells.2006-0432.
- <sup>22</sup>Katritsis, D. G., P. A. Sotiropoulou, E. Karvouni, I. Karabinos, S. Korovesis, S. A. Perez, E. M. Vouridis, and M. Papamichail. Transcoronary transplantation of autologous mesenchymal stem cells and endothelial progenitors into infarcted human myocardium. *Catheter Cardiovasc. Interv.* 65:321–329, 2005. doi:10.1002/ccd.20406.
- <sup>23</sup>Kinnaird, T., E. Stabile, M. S. Burnett, M. Shou, C. W. Lee, S. Barr, S. Fuchs, and S. E. Epstein. Local delivery of marrow-derived stromal cells augments collateral perfusion through paracrine mechanisms. *Circulation* 109:1543–1549, 2004. doi:10.1161/01.CIR.0000124062.31102.57.
- <sup>24</sup>Kobayashi, N., T. Yasu, H. Ueba, M. Sata, S. Hashimoto, M. Kuroki, M. Saito, and M. Kawakami. Mechanical stress promotes the expression of smooth muscle-like properties in marrow stromal cells. *Exp. Hematol.* 32:1238–1245, 2004. doi:10.1016/j.exphem.2004.08.011.
- <sup>25</sup>Kurpinski, K., J. Chu, C. Hashi, and S. Li. Anisotropic mechanosensing by mesenchymal stem cells. *Proc. Natl. Acad. Sci. U S A* 103:16095–16100, 2006. doi:10.1073/pnas.0604182103.
- <sup>26</sup>Liu, L., Z. Sun, B. Chen, Q. Han, L. Liao, M. Jia, Y. Cao, J. Ma, Q. Sun, M. Guo, Z. Liu, H. Ai, and R. C. Zhao. Ex vivo expansion and in vivo infusion of bone marrow-derived Flk-1+CD31-CD34- mesenchymal stem cells: feasibility and safety from monkey to human. *Stem Cells Dev.* 15:349–357, 2006. doi:10.1089/scd.2006.15.349.
- <sup>27</sup>Mohyeddin-Bonab, M., M. R. Mohamad-Hassani, K. Alimoghaddam, M. Sanatkar, M. Gasemi, H. Mirkhani, H. Radmehr, M. Salehi, M. Eslami, A. Farhig-Parsa, H. Emami-Razavi, M. G. al-Mohamad, A. A. Solimani, A. Ghavamzadeh, and B. Nikbin. Autologous in vitro expanded mesenchymal stem cell therapy for human old myocardial infarction. *Arch. Iran. Med.* 10:467–473, 2007.
- <sup>28</sup>Ohnishi, S., H. Sumiyoshi, S. Kitamura, and N. Nagaya. Mesenchymal stem cells attenuate cardiac fibroblast proliferation and collagen synthesis through paracrine actions.

- FEBS Lett.* 581:3961–3966, 2007. doi:10.1016/j.febslet.2007.07.028.
- <sup>29</sup>Oswald, J., S. Boxberger, B. Jorgensen, S. Feldmann, G. Ehninger, M. Bornhauser, and C. Werner. Mesenchymal stem cells can be differentiated into endothelial cells in vitro. *Stem Cells* 22:377–384, 2004. doi:10.1634/stemcells.22-3-377.
- <sup>30</sup>Park, J. S., J. S. Chu, C. Cheng, F. Chen, D. Chen, and S. Li. Differential effects of equiaxial and uniaxial strain on mesenchymal stem cells. *Biotechnol. Bioeng.* 88:359–368, 2004. doi:10.1002/bit.20250.
- <sup>31</sup>Pittenger, M. F., and B. J. Martin. Mesenchymal stem cells and their potential as cardiac therapeutics. *Circ. Res.* 95:9–20, 2004. doi:10.1161/01.RES.0000135902.99383.6f.
- <sup>32</sup>Potapova, I. A., G. R. Gaudette, P. R. Brink, R. B. Robinson, M. R. Rosen, I. S. Cohen, and S. V. Doronin. Mesenchymal stem cells support migration, extracellular matrix invasion, proliferation, and survival of endothelial cells in vitro. *Stem Cells* 25:1761–1768, 2007. doi:10.1634/stemcells.2007-0022.
- <sup>33</sup>Qiu, Q., M. Sayer, M. Kawaja, X. Shen, and J. E. Davies. Attachment, morphology, and protein expression of rat marrow stromal cells cultured on charged substrate surfaces. *J. Biomed. Mater. Res.* 42:117–127, 1998. doi:10.1002/(SICI)1097-4636(199810)42:1<117::AID-JBM15>3.0.CO;2-I.
- <sup>34</sup>Rana, O. R., C. Zobel, E. Saygili, K. Brixius, F. Gramley, T. Schimpf, K. Mischke, D. Frechen, C. Knackstedt, R. H. Schwinger, P. Schauerte, and E. Saygili. A simple device to apply equibiaxial strain to cells cultured on flexible membranes. *Am. J. Physiol. Heart Circ. Physiol.* 294:H532–H540, 2008. doi:10.1152/ajpheart.00649.2007.
- <sup>35</sup>Ries, C., V. Egea, M. Karow, H. Kolb, M. Jochum, and P. Neth. MMP-2, MT1-MMP, and TIMP-2 are essential for the invasive capacity of human mesenchymal stem cells: differential regulation by inflammatory cytokines. *Blood* 109:4055–4063, 2007. doi:10.1182/blood-2006-10-051060.
- <sup>36</sup>Simmons, C. A., S. Matlis, A. J. Thornton, S. Chen, C. Y. Wang, and D. J. Mooney. Cyclic strain enhances matrix mineralization by adult human mesenchymal stem cells via the extracellular signal-regulated kinase (ERK1/2) signaling pathway. *J. Biomech.* 36:1087–1096, 2003. doi:10.1016/S0021-9290(03)00110-6.
- <sup>37</sup>Song, G., Y. Ju, X. Shen, Q. Luo, Y. Shi, and J. Qin. Mechanical stretch promotes proliferation of rat bone marrow mesenchymal stem cells. *Colloids Surf. B Biointerfaces* 58:271–277, 2007. doi:10.1016/j.colsurfb.2007.04.001.
- <sup>38</sup>Sotoudeh, M., S. Jalali, S. Usami, J. Y. Shyy, and S. Chien. A strain device imposing dynamic and uniform equi-biaxial strain to cultured cells. *Ann. Biomed. Eng.* 26:181–189, 1998. doi:10.1114/1.88.
- <sup>39</sup>Sumanasinghe, R. D., S. H. Bernacki, and E. G. Lobo. Osteogenic differentiation of human mesenchymal stem cells in collagen matrices: effect of uniaxial cyclic tensile strain on bone morphogenetic protein (BMP-2) mRNA expression. *Tissue Eng.* 12:3459–3465, 2006. doi:10.1089/ten.2006.12.3459.
- <sup>40</sup>Wang, J. H., P. Goldschmidt-Clermont, and F. C. Yin. Contractility affects stress fiber remodeling and reorientation of endothelial cells subjected to cyclic mechanical stretching. *Ann. Biomed. Eng.* 28:1165–1171, 2000. doi:10.1114/1.1317528.
- <sup>41</sup>Wu, C. C., Y. S. Li, J. H. Haga, R. Kaunas, J. J. Chiu, F. C. Su, S. Usami, and S. Chien. Directional shear flow and Rho activation prevent the endothelial cell apoptosis induced by micropatterned anisotropic geometry. *Proc. Natl. Acad. Sci. U S A* 104:1254–1259, 2007. doi:10.1073/pnas.0609806104.
- <sup>42</sup>Wu, X., L. Huang, Q. Zhou, Y. Song, A. Li, J. Jin, and B. Cui. Mesenchymal stem cells participating in ex vivo endothelium repair and its effect on vascular smooth muscle cells growth. *Int. J. Cardiol.* 105:274–282, 2005. doi:10.1016/j.ijcard.2004.12.090.
- <sup>43</sup>Wu, X., L. Huang, Q. Zhou, Y. Song, A. Li, H. Wang, and M. Song. Effect of paclitaxel and mesenchymal stem cells seeding on ex vivo vascular endothelial repair and smooth muscle cells growth. *J. Cardiovasc. Pharmacol.* 46:779–786, 2005. doi:10.1097/01.fjc.0000187940.14102.64.
- <sup>44</sup>Wuchter, P., J. Boda-Heggemann, B. K. Straub, C. Grund, C. Kuhn, U. Krause, A. Seckinger, W. K. Peitsch, H. Spring, A. D. Ho, and W. W. Franke. Processus and recessus adhaerentes: giant adherens cell junction systems connect and attract human mesenchymal stem cells. *Cell Tissue Res.* 328:499–514, 2007. doi:10.1007/s00441-007-0379-5.